Order Parameter Description of Stationary Partially Fluidized Shear Granular Flows

Dmitri Volfson,[1] Lev S. Tsimring,[1] and Igor S. Aranson[2]
[1]*Institute for Nonlinear Science, University of California, San Diego, La Jolla, California 92093-0402, USA*
[2]*Argonne National Laboratory, 9700 South Cass Avenue, Argonne, Illinois 60439, USA*
(Received 23 December 2002; published 23 June 2003)

We carry out a detailed comparison of soft-particle molecular dynamics simulations with the theory of partially fluidized shear granular flows. We verify by direct simulations a constitutive relation based on the separation of the shear stress tensor into a fluid part proportional to the strain rate tensor, and a remaining solid part. The ratio of these two components is determined by the order parameter. Based on results of the simulations we construct the "free energy" function for the order parameter. We also present the simulations of the stationary deep 2D granular flows driven by an upper wall and compare it with the continuum theory.

DOI: 10.1103/PhysRevLett.90.254301 PACS numbers: 45.70.Cc, 45.70.Mg, 46.25.–y, 83.80.Fg

When the ratio of shear to normal stress in a packed granular matter exceeds a certain threshold value, the granular matter yields and a flow ensues. In the last few years there have been many experimental, numerical, and theoretical studies [1–12] that explored a broad range of granular flow conditions. While dilute granular flows can be well described by the kinetic theory of dissipative granular gases [13], dense granular flows still present significant difficulties for theoretical description. A continuum theory of slow dense granular flows based on the so-called associated flow rule was proposed in Ref. [14]. This description neglects the effects of the dry friction between the grains and works only in a fluidized state, so it cannot describe the hysteretic nature of the granular flow relevant for stick slips [2], avalanching [7], etc. A model based on a Newtonian stress-strain constitutive relation with density dependent viscosity was proposed in Refs. [3]. In this model, the viscosity diverges at the fluidization threshold when the density approaches the random close packing density of grains.

Recently we proposed a phenomenological order parameter (OP) description of the fluidization transition [15]. The OP specifies the ratio between solid and fluid parts of the stress tensor. The viscosity is defined as a ratio of the *fluid* part of the shear stress to the strain rate and remains finite at the fluidization threshold. This model yielded a good qualitative description of a broad variety of phenomena occurring in granular flows.

In this Letter we report on 2D soft-particle molecular dynamics (MD) simulations performed to validate and quantify our OP theory. To fit the equation for the OP and stress-strain relation we performed simulations of the granular flow in a thin Couette geometry. The obtained set of equations was used to calculate the stress and velocity profiles in a *different* system, a thick granular layer under nonzero gravity driven by a moving heavy upper plate.

The theory [15] is based on a standard momentum conservation equation and the incompressibility condition applicable for slow dense flows. To close the system, we assumed that the stress tensor σ is composed of two parts, a solid part σ^s, and a fluid part σ^f (taken in a purely Newtonian form)

$$\sigma^f_{ij} = p_f \delta_{ij} - \mu_f \dot{\gamma}_{ij}, \tag{1}$$

where p_f is the isotropic "partial" fluid pressure, and μ_f is the viscosity coefficient associated with the fluid stress tensor. We set the fluid part of off-diagonal components of the stress tensor to be proportional to the off-diagonal components of the full stress tensor with the proportionality coefficient being a function of the OP ρ,

$$\sigma^f_{yx} = q(\rho)\sigma_{yx}; \qquad \sigma^s_{yx} = [1 - q(\rho)]\sigma_{yx}. \tag{2}$$

We choose a fixed range for the OP such that it is zero in a completely fluidized state and one in a completely static regime. Thus, $q(0) = 1, q(1) = 0$. In Refs. [15] for simplicity we postulated $q(\rho) = 1 - \rho$. A similar relationship can be introduced for the diagonal terms of the stress tensor

$$\sigma^f_{xx} = q_x(\rho)\sigma_{xx}, \qquad \sigma^f_{yy} = q_y(\rho)\sigma_{yy}, \tag{3}$$

$$\sigma^s_{xx} = [1 - q_x(\rho)]\sigma_{xx}, \qquad \sigma^s_{yy} = [1 - q_y(\rho)]\sigma_{yy}. \tag{4}$$

The dynamics of the OP was assumed to be relaxational in nature and controlled by the generic Ginzburg-Landau equation

$$\frac{D\rho}{Dt} = D\nabla^2\rho - F(\rho, \delta). \tag{5}$$

Here D/Dt is the material derivative, D is the diffusion coefficient, and $F(\rho, \delta)$ is the derivative of the free energy density which has a quartic polynomial form to account for the bistability near the solid-fluid transition. Control parameter δ was taken to be a linear function of $\phi = \max|\sigma_{mn}/\sigma_{nn}|$.

The OP ρ which plays a pivotal role in the theory, should be associated with the "microscopic" properties of the granular assembly. At any moment of time all

contacts among the grains can be classified as either *fluidlike* or *solidlike*. A contact is considered fluidlike if two particles slide past each other or briefly collide and is solidlike if two particles are jammed together for longer than a characteristic collision time. Here we postulate that the OP can be introduced as a ratio between space-time averaged numbers of solid contacts $\overline{\langle Z_s \rangle}$ and all contacts $\overline{\langle Z \rangle}$ within a sampling area,

$$\rho(y) = \overline{\langle Z_s \rangle}/\overline{\langle Z \rangle}, \tag{6}$$

where $\langle \xi \rangle$ and $\overline{\xi}$ stand for averaging of ξ in space and time, respectively. This definition satisfies both limiting cases: when a granulate is in a solid state all contacts are stuck and $\rho = 1$; when it is strongly agitated $\overline{\langle Z_s \rangle}$ is zero and $\overline{\langle Z \rangle}$ is small but finite, and therefore $\rho = 0$. Our OP is expected to be sensitive to the degree of fluidization. A small rearrangement of the force network may result in strong fluctuations of ρ, while the solid fraction and granular temperature remain virtually constant. This quantity is difficult to measure in experiments; however, it can be found in soft-particle molecular dynamics.

Molecular dynamics simulations [16] were performed in two-dimensional geometry using a standard soft-particle algorithm similar to Refs. [9–11]. The grains are assumed to be noncohesive, dry, inelastic disklike particles which possess two translational and one rotational degrees of freedom. Two grains interact via normal and shear forces whenever they overlap. For the normal impact we employed the *spring-dashpot* model [10]. The model for shear force is based upon the technique developed in [17] which incorporates tangential elasticity and Coulomb laws of friction. For a detailed discussion of the advantages and limitations of the employed model, see Refs. [9–11]. The computational domain spans the $L_x \times L_y$ area, and is periodic in the horizontal direction x. The grain diameters are uniformly distributed around the mean with relative width Δ_r to avoid crystallization effects [9]. The material parameters of grains were chosen similar to Ref. [11]. All quantities are normalized by an appropriate combination of the average particle diameter d, mass m, and gravity g.

We studied a thin (50×10) granular layer sandwiched between two "rough plates" under fixed external pressure P_{ext} and zero gravity conditions. The rough plates were simulated by two straight chains of large grains "glued" together. Two opposite forces $\mathbf{F}_1 = -\mathbf{F}_2$ were applied to the plates along the horizontal x axis to induce shear stress in the bulk. We started with weak forces and slowly ramped them up and down in small increments. At every "stop" we measured all stress components, strain rate, and the OP by averaging over the whole layer and over time. These simulations were carried out at several values of the external pressure P_{ext}. Figure 1 shows ρ as a function of the normalized shear stress $\delta = -\sigma_{yx}/P_{\text{ext}}$. With this normalization, the results of several simulations with different P_{ext} collapse on a single bifurcation curve. We observe a quiescent state $\rho = 1$ until δ reaches a certain critical value $\delta_1 \approx 0.32$. This value differs slightly for different runs because of the finite system size and absence of self-averaging in the static regime. Above δ_1, ρ abruptly drops to approximately 0.15. At larger δ, the OP rapidly approaches zero. The return curve corresponding to the diminishing of the shear stress follows roughly the same path, and then continues to another (smaller) value of the shear stress, $\delta_2 \approx 0.23$. At this point the OP jumps back to one, and the granular layer returns to a jammed state. The striking feature of this bifurcation diagram is the hysteretic behavior of the OP as a function of the shear stress. Similar behavior was reported in [11] for the total fraction of sliding contacts and in [12] for the rigidity transition in granular packings. Assuming that there is an (unobserved) unstable branch of the bifurcation curve which merges with the stable branch at $\delta \approx \delta_1$, we make a simple analytic fit,

$$F(\rho, \delta) = (1 - \rho)\{\rho^2 - 2\rho_* \rho + \rho_*^2 \exp[-A(\delta^2 - \delta_*^2)]\} \tag{7}$$

with $\rho_* = 0.6$, $A = 25$, $\delta_* = 0.26$ (see Fig. 1, dashed line), and use it in Eq. (5). The inset of Fig. 1 depicts the density ν vs the OP ρ for the same runs. The density stays almost constant in a wide range of the OP $0.1 < \rho < 1$. This shows that, unlike the particle density, our OP is a sensitive characteristic of slow dense granular flows reflecting subtle changes in the contact network and the structure of the stress distribution.

We also probed the relaxation dynamics of the OP by studying the response of the system on small perturbation in the hysteretic region, $\delta_2 < \delta < \delta_1$ [16]. From these simulations we find that the intrinsic time scale of the OP relaxation is rather small, $O(1)$.

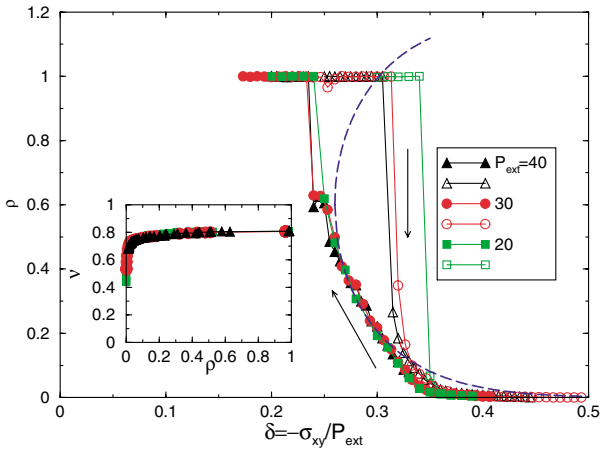

FIG. 1 (color online). ρ vs δ for $P_{\text{ext}} = 20$ (□), 30 (○), and 40 (△). Open symbols correspond to ramp-up, and filled symbols to ramp-down in shear stress. Dashed line shows fit to Eq. (7). Inset: density ν vs ρ for the same three P_{ext}.

The constitutive relation was fitted using the same Couette flow simulations. We analyzed the fluid stress σ^f_{ij} and the solid stress σ^s_{ij} separately during our ramp-down simulations at three different values of P. Figure 2 shows the ratios of fluid tensor components to the corresponding full tensor components as functions of ρ. We observe that data for $\sigma^s_{xy}/\sigma_{xy}$ and $\sigma^s_{yx}/\sigma_{yx}$ for different P fall onto a single curve which is fitted by $q(\rho) = (1-\rho)^{2.5}$ [Fig. 2(a)]. Repeating the procedure with diagonal elements yields different scaling; see Fig. 2(b). A small but noticeable difference is evident between $\sigma^f_{xx}/\sigma_{xx}$ and $\sigma^f_{yy}/\sigma_{yy}$. Detailed analysis shows that, in fact, fluid parts of the diagonal components of the stress tensor σ^f_{xx} and σ^f_{yy} are nearly identical [18], and the difference is mainly due to the solid part of the normal stresses. Functions $q_{x,y}(\rho)$ approach 1 as $\rho \to 0$, but they may have different functional form to reflect the anisotropy of the solid stress tensor. In our Couette flow, σ_{xx} and σ_{yy} can be fitted by $q_x(\rho) \approx (1-\rho)^{1.9}$ and $q_y(\rho) \approx (1-\rho^{1.2})^{1.9}$, respectively; see Fig. 2(b). We observe that even in a partially fluidized regime, the "fluid phase" component behaves as a fluid with a well-defined isotropic partial pressure p_f which is zero in a solid state and is becoming the full pressure in a completely fluidized state.

To test the stress-strain relation (1) we plot $-\sigma^f_{yx}$ vs $\dot\gamma_{yx}$; see Fig. 3. At small $\dot\gamma_{yx}$ all curves are close to the same straight line $\sigma^f_{yx} \approx 12\dot\gamma_{yx}$; i.e., the Newtonian scaling for fluid shear stress holds reasonably well. The deviations at large $\dot\gamma_{yx}$ are evidently caused by variations of density and temperature in the dilute regime as to be expected from the kinetic theory of dilute granular flows [13]. The full shear stress, of course, does not vanish as $\dot\gamma_{yx} \to 0$ (Fig. 3, inset). Therefore, the standard viscosity coefficient defined as the ratio of the full shear stress and strain rate diverges at the fluidization threshold as observed in Ref. [3].

We applied our theoretical description which was formulated above on the basis of MD simulations of a thin Couette flow with no gravity, to a *different* system, a shear granular flow in a thick granular layer under gravity driven by the upper plate which was pulled with constant speed V (or constant force F). A similar system has been studied experimentally in Refs. [2,8]. We simulated up to 20 000 particles in a periodic rectangular box under a heavy plate which was moved horizontally in the x direction. We systematically carried out a comparison between MD simulations and the continuum theory using the stress-strain relations and the specific form of the OP equation described above. We used no-flux boundary conditions for the OP and a no-slip condition for the velocity at the bottom plate. The boundary condition at the top plate where the flow can be in a dilute regime is a separate issue which we do not address here. We assumed that the shear stress component in the bulk is specified by applied force, and calculated the velocity profile using the constitutive relation (1)–(4). We found that the constitutive relations determined from the thin Couette experiment hold for this system as well. Furthermore, we ran several simulations with different values of restitution coefficient and rigidity of grains and, surprisingly, while the bulk order parameter dynamics were affected by these parameters, the constitutive functions $q(\rho)$, $q_i(\rho)$ were not. Selected results for the OP and velocity profiles are presented in Fig. 4. As seen from the figure, the vertical profiles of the OP and the horizontal velocities are reasonably well described by the theory. However, for low pressure the horizontal velocity profiles deviate from the numerical data for low pressure runs, apparently because

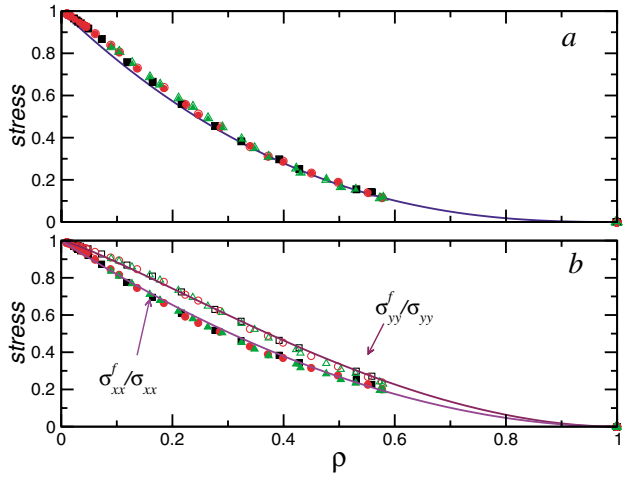

FIG. 2 (color online). Ratios of the fluid stress components to the full stress components $\sigma^f_{ij}/\sigma_{ij}$ vs ρ for $P_{\rm ext} = 20$ (□), 30 (○), and 40 (△). (a) Shear stress components σ_{yx} (open symbols), σ_{yx} (filled symbols), line is a fit $q(\rho) = (1-\rho)^{2.5}$. (b) Normal stress components σ_{xx} (closed symbols), σ_{yy} (open symbols), lines are the fits $q_x(\rho) = (1-\rho)^{1.9}$, $q_y(\rho) = (1-\rho^{1.2})^{1.9}$.

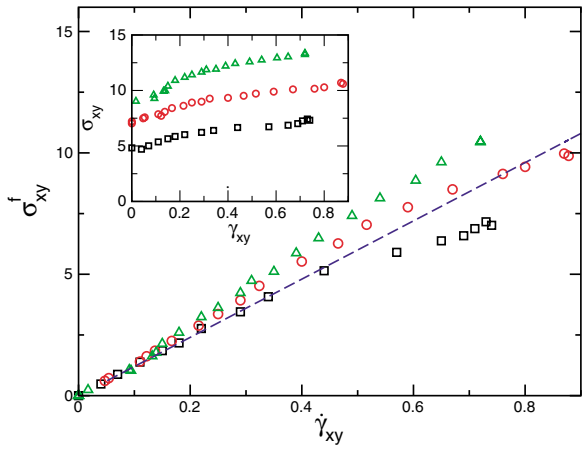

FIG. 3 (color online). Stress-strain rate relation for a thin granular Couette flow at $P_{\rm ext} = 20$ (□), 30 (○), and 40 (△). Fluid shear stress vs strain rate, the straight line is a constant viscosity fit $\sigma^f = 12\dot\gamma$. Inset: full shear stress vs strain rate.

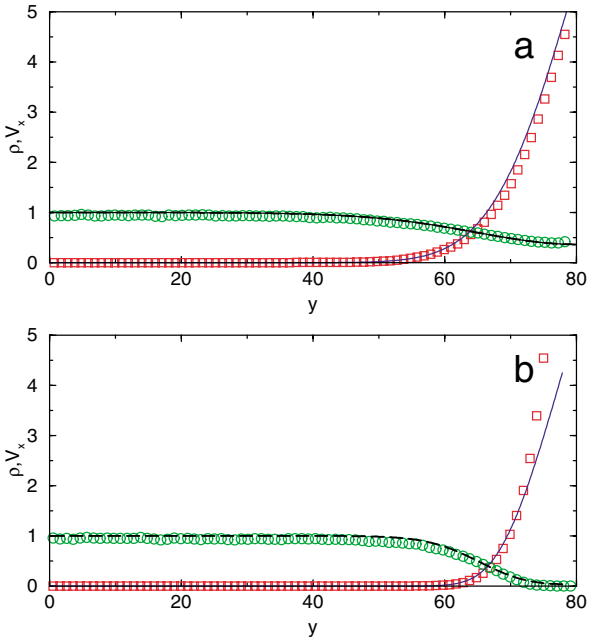

FIG. 4 (color online). Vertical profiles of ρ and V_x in a thick granular layer driven at the surface by a heavy plate for 5000 particles, in the box $L_x = 50$, $L_y = 100$, (a) $P_{\text{ext}} = 50$, pulling velocity $V = 5$, $D = 5$, (b) $P_{\text{ext}} = 10$, pulling velocity $V = 50$, $D = 1$. Lines show the theoretical results obtained from the continuum model (5) and (7); open symbols show numerical data.

the viscosity coefficient is no longer a constant in a dilute region near the top plate. The only fitting parameter used was the diffusion constant D in the OP equation, which has not been determined in our simulations of the thin layer. It appears that the diffusion coefficient depends on the applied pressure and the strain rate; however, more detailed numerical experiments are needed.

In conclusion, we calibrated the theory of partially granular flows [15] on the basis of a series of 2D soft-particle molecular dynamics simulations. The OP which controls the fluidization transition, was defined as the fraction of solidlike contacts among particles. Measurements of the OP, the stress tensor, and the strain rate in a thin Couette cell with no gravity, when all these quantities are uniform across the layer, allowed us to quantify the constitutive relations based on the relaxational OP dynamics. Then we studied the nonuniform flow structure of a thick surface driven granular flow under gravity and found the model predictions to be in a good *quantitative* agreement with soft-particle MD simulations. Our results support an intriguing interpretation for the OP description of dense and slow granular flows. The granular matter under shear stress appears to be similar to a multiphase system with the fluid phase "immersed" in the solid phase. The fluid phase behaves as a simple Newtonian fluid for small shear rates when the density is almost constant, but exhibits shear thinning at larger shear rates when the density begins to drop. This regime can be described by the generalization of the theory [16] which includes the equations for density and granular temperature following from the kinetic theory of dilute granular gases. Our simulations were limited to 2D geometry. While we anticipate that the structure of the model should remain unchanged in 3D systems, the specific form of the fitting functions may vary.

The authors are indebted to J. Gollub, P. Cvitanovic, T. Halsey, and B. Behringer for useful discussions, and to J.C. Tsai for sharing his unpublished experimental data. This work was supported by the Office of the Basic Energy Sciences at the U.S. DOE, Grants No. W-31-109-ENG-38 and No. DE-FG03-95ER14516. Simulations were performed at the National Energy Research Scientific Computing Center.

[1] C. T. Veje, D. W. Howell, and R. P. Behringer, Phys. Rev. E **59**, 739 (1999).
[2] S. Nasuno, A. Kudrolli, A. Bak, and J. P. Gollub, Phys. Rev. E **58**, 2161 (1998).
[3] W. Losert, L. Bocquet, T. C. Lubensky, and J. Gollub, Phys. Rev. Lett. **85**, 1428 (2000); L. Bocquet, W. Losert, D. Schalk, T. C. Lubensky, and J. P. Gollub, Phys. Rev. E **65**, 011307 (2002); L. Bocquet, J. Errami, and T. C. Lubensky, Phys. Rev. Lett. **89**, 184301 (2002).
[4] A. Lemaitre, Phys. Rev. Lett. **89**, 064303 (2002); **89**, 195503 (2002).
[5] L. Staron, J.-P. Vilotte, and F. Radjai, Phys. Rev. Lett. **89**, 204302 (2002).
[6] O. Pouliquen, Phys. Fluids **11**, 542 (1999).
[7] A. Daerr and S. Douady, Nature (London) **399**, 241 (1999); A. Daerr, Phys. Fluids **13**, 2115 (2001).
[8] J. C. Tsai, G. Voth, and J. P. Gollub (unpublished).
[9] P. A. Thompson and G. S. Grest, Phys. Rev. Lett. **67**, 1751 (1991).
[10] J. Schäfer, S. Dippel, and D. E. Wolf, J. Phys. I (France) **6**, 5 (1996); H. J. Herrmann and S. Luding, Continuum Mech. Thermodyn. **10**, 189–231 (1998); A. Dziugys and B. Peters, Granular Matter **3**, 231–266 (2001).
[11] L. E. Silbert *et al.*, Phys. Rev. E **64**, 051302 (2001); L. E. Silbert *et al.*, Phys. Rev. E **65**, 051307 (2002).
[12] E. Aharonov and D. Sparks, Phys. Rev. E **60**, 6890–6896 (1999); **65**, 051302 (2002).
[13] J. T. Jenkins and M. W. Richman, Phys. Fluids **28**, 3485 (1985).
[14] S. B. Savage, J. Fluid Mech. **377**, 1 (1998).
[15] I. S. Aranson and L. S. Tsimring, Phys. Rev. E **64**, 020301 (2001); **65**, 061303 (2002).
[16] D. Volfson, L. S. Tsimring, and I. S. Aranson, cond-mat/0302340[Phys. Rev. E (to be published)].
[17] P. A. Cundall and O. D. L. Strack, Geotechnique **29**, 47 (1979).
[18] In the dilute limit granular gases exhibit anisotropy of the normal stress components due to inelasticity, J. T. Jenkins and R. W. Richman, J. Fluid Mech. **192**, 313 (1988).